20122410 9A

厚生労働科学研究費補助金

障害者対策総合研究事業

アンチセンスによる筋強直性ジストロフィーの治療の最適化

平成 24 年度　総括・分担研究報告書

主任研究者　石浦　章一

平成 25（2013）年 4 月

目次

厚生労働科学研究費補助金（障害者対策研究事業）
総括研究報告書

筋強直性ジストロフィーの治療の最適化

総括研究者　　石浦章一　東京大学大学院 総合文化研究科　教授

研究要旨

筋強直性ジストロフィー１型(DM1)は、筋強直、精巣萎縮、白内障、耐糖能異常などを主徴とする全身性疾患であり、症状は遺伝子のスプライシングがおかしくなるため、と考えられている。私たちは塩素チャネル遺伝子をモデルとして遺伝子異常と症状との関係を調べ、バブル・リポソーム法を用いてアンチセンスを効率よく筋肉内に導入する計画を立てた。その結果、塩素チャネル遺伝子のスプライシングが正常化するとともに、症状であるミオトニアが軽減した。

分担研究者：西野一三

国立精神・神経医療研究センター神経研究所・部長

A．研究目的

筋強直性ジストロフィー１型(DM1)の原因は、第19染色体にあるDMPK遺伝子の3’非翻訳領域にあるCTGリピートの伸長で、症状は、筋強直（ミオトニア）、精神遅滞、精巣萎縮、白内障、耐糖能異常などの全身性である。分子レベルでは、数多くの遺伝子のスプライシングが異常になっており、このために全身症状が出現すると考えられている。本症は我が国の筋ジストロフィーの中では一番多く、筋力低下やミオトニアなどの治療法の開発が望まれていて、QOLの改善が最終目標である。

平成23年度は、塩素チャネル遺伝子を指標に、スプライシングを正常化させるアンチセンスを効率良く筋肉に導入する方法の開発に力を注いだ。また平成24年度は、アンチセンスの効果をモデル動物のミオトニアという指標によって評価した。また、塩素チャネルではなく、CTG のアンチセンスを用いることによって、全身で起こるスプライシングの異常を正常化することも試みた。

B．研究方法（倫理面の配慮含む）

・アンチセンス投与法

人工的に作成した塩素チャネル・ミニ遺伝子（エキソン 6、7A、7 でできている短い遺伝子）を用いて、エクソン 7A の有無を定量するスプライシングアッセイを行った。エクソン 7A がない成人（正常）型と、エクソン 7A を含む幼若（異常）型の比率は、正常筋では圧倒的に前者が多く、DM 筋では後者が増えている。エクソン 7A の 0～25 をコードするモルフォリノアンチセンスオリゴを、塩素チャネル・ミニ遺伝子とともに CTG300 を持つトランスジェニックマウス HAS-LR の tibialis anterior (TA)筋に 1 回注射した。このときのアンチセンス配列は、エクソン 7A の 0～25 に対するものであり、細胞系では最もエクソン 7a スキッピングが起こりやすくなるものである。最後の注射から 2 日後に、mRNA を抽出し、スプライシング頻度を測定した。このとき、モルフォリノオリゴ(10μg)はバブル・リポソームとともに筋注した（全 30μl)。その後、0-3 Wの出力で超音波を 0.5-3 分照射し、筋内にアンチセンスを導入した。

アンチセンスの効果は、ミオトニアの定量で行った。また、CTG に対するアンチセンスは、vivo モルフォリノを用いた。

（倫理面への配慮）

今回の実験は、DM 患者生検筋からの mRNA スプライシング異常から派生した研究である。生検筋は、インフォームドコンセントを得て取得し、国立精神･神経医療研究センター倫理委員会で承認

を受けたものを用いている。

C．研究結果

前年度の研究より、バブル・リポソームを用いるデリバリー法の場合、1Wの出力で超音波を1分間照射が最適条件であることが分かっているので、今回はこの条件を用いた。

その結果、エクソン7Aの挿入した幼若型の塩素チャネルの発現が25%に低下していることが分かった。また、マウス塩素チャネルに対する抗体で染色した結果、変異マウスでは細胞膜に局在しているものは少なく、パッチ状に存在していた。アンチセンス投与後は、きれいに細胞膜局在が見られた。

このとき、マウスのミオトニアが治るかどうかも検討した。筋電図によれば、ミオトニアの継続時間が低下し、明らかに症状軽減の効果が認められた。

次に、CTGリピートに対するCAGアンチセンスを同様に投与したところ、塩素チャネルのスプライシングが正常化したが、その割合は塩素チャネルアンチセンスに比べて少なかった。また、アンチセンスの効果にリピートの長さが関係していることが判明し、最適化には多くの条件検討が必要であることも明らかになった。

D．考察

平成24年度の研究では、アンチセンスを用いることによって、ミオトニアという症状も軽くなるということが分かった。これは臨床研究にとって重要で、スプライシングが正常化するだけではなく、症状も治ることがわかったのである。また、単なる筋注よりも、バブル・リポソームを用いた方がアンチセンス導入の効率が良いことが明らかになった。

一方、本症では多くの症状が一度に出ており、ミオトニアだけを治療しても完治したとは言えない。そこで、最終年度に向けて病気の本質を断ち切るCTGに対するアンチセンス導入の検討も行った。条件検討が難しかったが、CAGの長さが短い方がアンチセンス効果が高いことが判明した。

E．結論

新しいアンチセンスとバブル・リポソームに組み合わせにより、筋強直性ジストロフィーのモデルであるCTGリピートを300含むトランスジェニックマウスHAS-LRに対して、有効な治療効果を得ることができた。また、スプライシングを正常化するだけではなく、ミオトニア症状までも軽くなることが分かった。今後は、CTGに対するアンチセンス治療の条件を検討し、臨床治験に向けての最適化を図りたい。

F．健康危険情報

なし

G．研究発表

1．論文発表

(1) Zhao, Y., Koebis, M., Suo, S., Ohno, S. & Ishiura, S. (2012) Regulation of *SERCA1* alternative splicing by PMA through PKC pathway. Biochem. Biophys. Res. Commun. 423, 212-217

(2) Sato, K., Tanabe, C., Yonemura, Y., Watahiki, H., Zhao, Y., Yagishita, S., Ebina, M., Suo, S., Futai, E., Murata, M. & Ishiura, S. (2012) Localization of mature neprilysin in lipid rafts. J. Neurosci. Res. 90, 870-877

(3) Kanno, K. & Ishiura, S. (2012) The androgen receptor facilitates inhibition of human *dopamine transporter* (*DAT1*) reporter gene expression by HESR1 and HESR2 via the variable number of tandem repeats. Neurosci. Lett. 525, 54-59

H．知的財産権の出願・登録状況

なし

厚生労働科学研究費補助金（障害者対策研究事業）
分担研究報告書

筋強直性ジストロフィーの治療の最適化

研究分担者　西野　一三　　（独）国立精神・神経医療研究センター神経研究所　部長

研究要旨

先天性筋強直性ジストロフィーはタイプ1線維がタイプ2線維より小径（12%以上の差）という病理所見で定義づけられる先天性ミオパチーである先天性筋線維タイプ不均等症(CFTD)類似の所見を呈することがある。従って、CFTDの鑑別を十分に検討することが正確な診断に繋がる。今年度は、乳幼児期に発症したCFTDに類似した筋病理所見を呈するミオパチーを、*RYR1*複合ヘテロ接合型の例で見出した。その臨床像、病理像において先天性筋強直性ジストロフィーとの相違について検討を行った。その結果、先天性筋強直性ジストロフィー同様に、筋力低下は成長（加齢）とともに軽快してくるが、顔面筋罹患や外眼筋麻痺、CK低値を示すものではRYR1遺伝子を考慮すべきであることが明らかになった。

A．研究目的

我々はこれまでに、先天性筋強直性ジストロフィーが臨床病理学的に、先天性ミオパチーのなかのミオチュブラーミオパチーや、先天性筋線維タイプ不均等症(CFTD)類似の筋病理所見を呈することを示してきた。このことは、ミオチュブラーミオパチーや CFTD の鑑別診断を十分に検討することが、先天性筋強直性ジストロフィーの正確な診断に繋がることを示している。昨年度はその検討の 1 つとして、CFTD 様の病理所見を呈する症例の中から、核膜蛋白質 A 型ラミンをコードする LMNA 遺伝子変異による *LMNA* ミオパチーの例を見出し、臨床・筋病理学的な特徴を明らかにしたが、いまだ多くの例では責任遺伝子が同定されていない。今年度は、筋小胞体 Ca^{++}遊離チャネルであるリアノジン受容体をコードする RYR1 遺伝子変異に着目し、変異未確定の CFTD 所見を呈するミオパチー症例の検討を行った。

RYR1 遺伝子は染色体 19q13 上に存在し、その蛋白質であるリアノジン受容体は、筋小胞体膜のカルシウム調整チャネルとして作用し、骨格筋の筋収縮連関に関与する。これまで、悪性高熱症患者での遺伝子変異が同定されているほか、先天性ミオパチーのなかのセントラルコア病の責任遺伝子としても知られている。近年、マルチコア病、中心核病など、他の先天性ミオパチーでの報告も散見され、先天性ミオパチーのなかで比較的多く認められる変異ではないか、とも言われている。悪性高熱症患者は日常生活では無症状であるが、誘発薬を投与されることにより発症し、一度発症すると症状は急激に悪化し死に至る。筋病理所見はほぼ正常で特有の所見は認めない。セントラルコア病は、軽度の筋力低下のほか側彎を認めるが、生命予後としては良好な疾患である。筋病理では、NADH-TR 染色で筋線維の中心部がコア様に抜け染色されない特徴的な所見がみられ、同じ *RYR1* 変異でも、その表現型は異なる。

先天性筋線維タイプ不均等症(CFTD)は筋病理所見で、タイプ 1 線維がタイプ 2 線維より小径（12%以上の差）であることを特徴とする先天性ミオパチーである。悪性高熱症やセントラルコア病で認めるような筋病理所見と CFTD では、筋病理学的に全く異なっているにも関わらず、今回我々は、乳幼児期に発症した CFTD 類似の所見を呈する *RYR1* ミオパチーを見出したため、臨床、筋病理学的な検討を行った。

B．研究方法（倫理面の配慮含む）

国立精神・神経医療研究センター骨格筋レポジトリーに登録されている先天性ミオパチー症例 746 例のうち、筋病理学的に CFTD が示唆された

94 例(CFTD 群)を対象とし、臨床像、臨床病理、遺伝学的解析を行った。

（倫理面への配慮）

今回の実験は、先天性筋強直性ジストロフィー患者生検からの mRNA スプライシング異常から派生した研究である。生検筋は、インフォームドコンセントを取得し国立精神・神経医療研究センター倫理委員会で承認を受けたものを用いる。

C．研究結果

CFTD 群のうち 6 例に RYR1 遺伝子変異を複合ヘテロ接合型で認めた。この 6 例の発症はいずれも生下時あるいは乳幼児期で、筋病理学的に診断されたのは 0 歳 6 ヵ月から 4 歳（平均 1 歳 9 ヵ月）であった。出生時は、フロッピーインファントといった筋力・筋緊張低下を呈し、また呼吸障害も認め、人工呼吸器または酸素投与が行われている。しかし、その後の成長（加齢）とともに軽快し、1 例を除いて人工呼吸器や酸素投与からの離脱が可能であった。運動発達も遅れを認めながらも、3 例で歩行獲得まで認めている。また顔面筋罹患は顕著で、外眼筋麻痺をも認めていた。血清 CK 値は、54±21 IU/L (基準値 45-163)と基準値内ではあるが低値を示した。筋病理所見から計算した fiber size disproportion (%FSD) [(mean type2 fiber diameter)-(mean type1 fiber diameter)/ mean type 2 fiber diameter] ×100 は 56.2±5.1%であり、ほかの筋病理所見として、内在核や非典型的なコア構造を示す例も散見された。

D．考察

今回同定し得た *RYR1* 複合ヘテロ接合型の CFTD 類似例は、同様の *RYR1* 変異である悪性高熱症やセントラルコア病の表現型とは全く異なり、成長に伴い人工呼吸器からの離脱が可能であるなど、むしろ先天性筋強直性ジストロフィーに類似の臨床症状を示していた。筋病理上のほか、臨床症状においても類似する点があるが、顔面筋罹患や外眼筋麻痺といった臨床所見や、CK 値が低値である点は、RYR1 遺伝子を考慮すべき所見であると考える。

E．結論

RYR1 複合ヘテロ接合型の例は、先天性筋強直性ジストロフィーと筋病理学的にも臨床症状においても共通する点を認める。このことから病因としては互いに近い位置にある可能性があり、筋病理の萎縮、大小不同をきたすメカニズム等の更なる分子生物学的解析が病態解明に結びつくものと考える。

F．健康危険情報

なし

G．研究発表

1．論文発表

1. Matsuda C, Miyake K, Kameyama K, Keduka E, Takeshima H, Imamura T, Araki N, Nishino I, Hayashi YK: The C2A domain in dysferlin is important for association with MG53 (TRIM 72). PLoS Curr. 4:e5035add8caff4. Nov, 2012

2. Mori-Yoshimura M, Okuma A, Oya Y, Fujimura-Kiyono C, Nakajima H, Matsuura K, Takemura A, Malicdan MC, Hayashi YK, Nonaka I, Murata M, Nishino I: Clinicopathological features of centronuclear myopathy in Japanese populations harboring mutations in dynamin 2. Clin Neurol Neurosurg. 114(6): 678-683. Jul, 2012.

2．学会発表

1. Ishiyama A, Hayashi YK, Kajino S, Komaki H, Saito T, Saito Y, Nakagawa E,

Sugai K, Sasaki M, Noguchi S, Nonaka I, Nishino I: Congenital fiber type disproportion with myofibrillar disorganization and altered internal nuclei is caused by *RYR1* mutation. 17th International Congress of the World Muscle Society. Perth, Australia, 10.9-10.13, 2012

2. Ishiyama A, Hayashi YK, Kajino S, Komaki H, Sugai K, Sasaki M, Noguchi S, Nonaka I, Nishino I: Congenital fiber type disproportion with myofibrillar disorganization and altered internal nuclei is caused by RYR1 mutation. The 11th Annual Meeting of the Asian and Oceanian Myology Center. Kyoto, 6.6-6.8, 2012

3. 石山昭彦，林由起子，小牧宏文，齋藤貴志，斎藤義朗，中川栄二，須貝研司，佐々木征行，西野一三：内在核と筋原線維間網の異常を有し二峰性筋線維不均等を示す先天性ミオパチーはRYR1変異が原因である．第54回日本小児神経学会総会，札幌，5.17-5.19, 2012

H．知的財産権の出願・登録状況

1．特許取得

特になし

2．実用新案登録

特になし

3．その他

特になし

別紙４

研究成果の刊行に関する一覧表

雑誌

発表者氏名	論文タイトル名	発表誌名	巻号	ページ	出版年
Zhao, Y., Koebis, M., Suo, S., Ohno, S. & Ishiura, S.	Regulation of *SERCA1* alternative splicing by PMA through PKC pathway.	Biochem. Biophys. Res. Commun.	423	212-217	2012
Sato, K., Tanabe, C., Yonemura, Y., Watahiki, H., Zhao, Y., Yagishita, S., Ebina, M., Suo, S., Futai, E., Murata, M. & Ishiura, S.	Localization of mature neprilysin in lipid rafts.	J. Neurosci. Res.	90	870-877	2012
Kanno, K. & Ishiura, S.	The androgen receptor facilitates inhibition of human *dopamine transporter* (*DAT1*) reporter gene expression by HESR1 and HESR2 via the variable number of tandem repeats.	Neurosci. Lett.	525	54-59	2012

別紙４

研究成果の刊行に関する一覧表

雑誌

発表者氏名	論文タイトル名	発表誌名	巻号	ページ	出版年
Matsuda C, Miyake K, Kameyama K, Keduka E, Takeshima H, Imamura T, Araki N, Nishino I, Hayashi YK	The C2A domain in dysferlin is important for association with MG53 (TRIM 72).	PLoS Curr.	4	e5035add8caff4	2012
Mori-Yoshimura M, Okuma A, Oya Y, Fujimura-Kiyono C, Nakajima H, Matsuura K, Takemura A, Malicdan MC, Hayashi YK, Nonaka I, Murata M, Nishino I	Clinicopathological features of centronuclear myopathy in Japanese populations harboring mutations in dynamin 2.	Clin Neurol Neurosurg.	114(6)	678-683	2012

Biochemical and Biophysical Research Communications 423 (2012) 212–217

Contents lists available at SciVerse ScienceDirect

Biochemical and Biophysical Research Communications

journal homepage: www.elsevier.com/locate/ybbrc

Regulation of the alternative splicing of *sarcoplasmic reticulum* Ca^{2+}-*ATPase1* (*SERCA1*) by phorbol 12-myristate 13-acetate (PMA) via a PKC pathway

Yimeng Zhao [a], Michinori Koebis [a], Satoshi Suo [a], Shigeo Ohno [b], Shoichi Ishiura [a,*]

[a] Department of Life Sciences, Graduate School of Arts and Sciences, The University of Tokyo, 3-8-1 Komaba, Meguro-ku, Tokyo 153-8902, Japan
[b] Department of Molecular Biology, Yokohama City University Graduate School of Medical Science, 3-9 Fuku-ura, Kanazawa-ku, Yokohama 236-0004, Japan

ARTICLE INFO

Article history:
Received 6 May 2012
Available online 15 May 2012

Keywords:
Myotonic dystrophy
Sarcoplasmic/endoplasmic reticulum
Ca^{2+}-ATPase 1 (SERCA1)
Alternative splicing
PKC
Phorbol 12-myristate 13-acetate (PMA)
CUG-binding protein 1 (CUGBP1)

ABSTRACT

Myotonic dystrophy type 1 (DM1) is a multi-systemic disease with no established treatment to date. Small, cell-permeable molecules hold the potential to treat DM1. In this study, we investigated the association between protein kinase C (PKC) signaling and splicing of *sarcoplasmic reticulum* Ca^{2+}-*ATPase1* (*SERCA1*). Our aim was to clarify the mechanisms underlying the regulation of alternative splicing, in order to explore new therapeutic strategies for DM1. By assessing the splicing pattern of the endogenous *SERCA1* gene in HEK293 cells, we found that treatment with phorbol 12-myristate 13-acetate (PMA) regulated *SERCA1* splicing. Interestingly, treatment with PMA for 48 h normalized *SERCA1* splicing, while treatment for 1.5 h promoted aberrant splicing. These two responses showed dose dependency and were completely abolished by the PKC inhibitor Ro 31-8220. Furthermore, repression of PKCβII and PKCθ by RNAi mimicked prolonged PMA treatment. These results indicate that PKC signaling is involved in the splicing of *SERCA1* and provide new evidence for a link between alternative splicing and PKC signaling.

1. Introduction

Myotonic dystrophy type 1 (DM1) is an inherited multi-systemic disorder caused by the aberrant expansion of CTG repeats in the *myotonic dystrophy protein kinase* (*DMPK*) 3′-untranslated region (3′-UTR). The clinical presentation of DM1 is highly variable, involving multiple organs, with symptoms including myotonia, cataracts, cardiac conduction defects, progressive muscle wasting and weakness, insulin resistance, and mental retardation. DM1 is a progressive disease; its symptoms become severe with age and across generations.

One reason why aberrantly expanded CTG repeats cause such diverse symptoms is explained by the RNA gain-of-function theory [1]. Expanded CTG repeats are transcribed into RNA with expanded CUG repeats, which possess muscleblind-like protein 1 (MBNL1) binding motifs. MBNL1 is a splicing factor that regulates alternative splicing in several genes (*Clcn1*, *IR*, *cTNT2*, and *SERCA1*) to normalize DM1 splicing abnormalities [2–4]. Ablation of MBNL1 function leads to mis-splicing of several genes. In addition, MBNL1-knockout mice show DM1-like splicing abnormalities and myotonia in their skeletal muscles [5,6]. Moreover, MBNL1-included foci, formed in the nuclei as a result of expanded CUG repeats, were observed by fluorescent immunostaining [3,7]. Thus, levels of free MBNL1 in the cytosol can be decreased by long CUG repeats. Without regulation by MBNL1, the alternative splicing of multiple genes becomes abnormal. Abnormally spliced transcripts are degraded by the nonsense-mediated mRNA decay (NMD) system or translated into abnormal proteins, thereby leading to DM1 symptoms.

Due to the diverse symptoms affecting multiple organs in DM1, its treatment has been limited to supportive care; no basic remedy has been developed. One possible basic remedy is the use of antisense nucleotides to alter the splicing patterns of genes that are aberrantly and indirectly regulated by CUG repeats. However, this method can only treat one gene-derived symptom at a time and requires a great deal of time and effort. Thus, two treatment strategies have been devised: antisense nucleotides against CUG repeats and small molecules. The first strategy uses antisense nucleotides to target CUG repeats and thereby cause repeats to segregate [8], repress [9], or dissolve [10]. However, how to deliver antisense nucleotides into living cells and achieve continual administration remains to be resolved. The other strategy is pharmacological therapy using small molecules. This method can resolve cell permeabilization problems. TG003 has been identified as a compound that improves normal splicing in Duchenne muscular dystrophy (DMD) [11]. In DM1, similarly effective treatment is expected [12,13].

SERCA1 is an aberrantly spliced gene in DM1. SERCA1 protein regulates intracellular Ca^{2+} homeostasis in skeletal muscle cells. The switching of SERCA1 from a fetal isoform, SERCA1b (lacking

Abbreviations: SERCA1, *sarcoplasmic reticulum* Ca^{2+}-*ATPase1*; PMA, phorbol 12-myristate 13-acetate; DM1, myotonic dystrophy type 1; DMPK, myotonic dystrophy protein kinase; MBNL1, muscleblind-like protein 1; CUGBP1, CUG-binding protein 1; CELF, CUG-BP and ETR-3-like (embryonic lethal abnormal vision-type RNA-binding protein 3-like) factor.

* Corresponding author.
E-mail address: cishiura@mail.ecc.u-tokyo.ac.jp (S. Ishiura).

0006-291X/$ - see front matter © 2012 Elsevier Inc. All rights reserved.
http://dx.doi.org/10.1016/j.bbrc.2012.05.033

exon 22), to a mature isoform, SERCA1a (which contains exon 22), is thought to play a central role in muscle development. Since exon 22 contains a stop codon, SERCA1b is six amino acid residues longer than SERCA1a. No specific protein structure has been identified in this six-amino acid residue region [14]. However, in normal skeletal muscle tissues, the expression of *SERCA1a* is strictly regulated [4]; *SERCA1b* is only detected in DM1 patients. Other studies have reported that extended, injured, and fetal muscles express *SERCA1b* [15,16]. Determining the differences between the two isoforms of SERCA1 and their functions is important to our understanding of the DM1 pathogenesis. Expression of *SERCA1b* in DM1 patients indicates that there is some deficiency in this pattern-shift point or in myogenesis. MBNL1 has been identified as a splicing factor that regulates the alternative splicing of *SERCA1* and promotes the production of *SERCA1a* [4]. In this report, we attempted to clarify the mechanisms underlying *SERCA1* splicing to determine the pathogenesis of DM1.

Approximately 500 kinds of protein kinases are involved in signal transduction. Collectively, they regulate diverse cell events, including apoptosis, mitosis, and responses to exogenous stimulators. In the present study, we found that prolonged treatment with phorbol 12-myristate 13-acetate (PMA) normalized *SERCA1* splicing. PMA is a well-known protein kinase C (PKC) activator that imitates diacylglycerol (DAG) and binds to the C1A and C1B domains of PKC isozymes. However, prolonged stimulation with PMA downregulates PKC, thereby inhibiting PKC activation.

PKC regulates various cellular processes including apoptosis, cell division, and cell proliferation. This class of serine/threonine-specific protein kinases can be divided into three groups according to basic structure: conventional PKCs (cPKCs), novel PKCs (nPKCs), and atypical PKCs (aPKCs). The cPKCs (PKCα, PKCβI, PKCβII, and PKCγ contain C1A and C1B domains (DAG binding site) and a C2 domain (Ca^{2+} binding site). The nPKCs (PKCδ, PKCε, PKCη, PKCθ, PKCμ, and PKCν) contain only C1A and C1B domains. The aPKCs (PKCξ and PKCι) have no special DAG or Ca^{2+} binding domains. In the normal state, PKC isozymes are usually inactivated by self-inhibitory effects. cPKC isozymes require Ca^{2+}, DAG, and phosphatidyl serine (PS) for activation, while nPKCs are Ca^{2+}-independent and aPKCs can be activated by PS alone.

The association between DM1 pathogenesis and PKC has been described in two reports. CUG-binding protein 1 (CUGBP1) belongs to the CUG-BP and ETR-3-like (embryonic lethal abnormal vision-type RNA-binding protein 3-like) factor (CELF) family and is one of the key factors inducing aberrant splicing in DM1 (*CLC1*, *cTNT* [17] and *Ca(V)1.1* [18]). It is hyperphosphorylated by CUG repeats and promotes an increase in the steady-state level of CUGBP1. In addition, PKC activation is required for this hyperphosphorylation. Specifically, PKCα and PKCβII have been shown to directly activate CUGBP1 *in vitro* [19]. Furthermore, administration of the PKC inhibitor Ro 31-8220 to DM1 model mice ameliorated cardiac conduction defects in DM1 [20].

In this report, we describe a series of experiments that explored the properties of PKC-mediated alternative splicing using the PKC activator PMA and the PKC inhibitor Ro 31-8220. By exploring the mechanisms regulating the splicing of *SERCA1*, we found that PKCβII and PKCθ were involved in the regulation of *SERCA1* splicing. This report identifies a new regulator of *SERCA1* splicing and a therapeutic strategy for DM1.

2. Materials and methods

2.1. PMA treatment and RT-PCR

HEK293 cells were cultured in Dulbecco's modified Eagle's medium (DMEM) containing 10% fetal bovine serum (FBS) and incubated in an atmosphere containing 5% CO_2 at 37 °C. PMA (final concentration, 5–500 nM) was applied for between 5 min and 48 h. Concentrations of PMA higher than 500 nM induced cell death at 48 h.

Cells were washed with 1 × PBS before cultivation. Total cellular RNA was purified using a GenElute Mammalian Total RNA Miniprep kit (Sigma–Aldrich, MO, USA). Next, 2.5 μg of total RNA was reverse transcribed using a PrimeScript 1st Strand cDNA Synthesis kit (TAKARA BIO, Shiga, Japan) and oligo(dT) primers. *SERCA1* was used to assess the compound's ability to alter splicing patterns. Exons 21 to 23 of endogenous *SERCA1* were amplified by PCR using the following primers: forward, 5′-ATC TTC AAG CTC CGG GCC CT-3′; reverse, 5′-CAG CTC TGC CTG AAG ATG TG) [4]. The annealing temperature was 63.5 °C and there were 30 amplification cycles. PCR products were separated by electrophoresis in an 8% polyacrylamide gel, stained with ethidium bromide, and analyzed using an LAS-3000 luminescence image analyzer (Fujifilm, Tokyo, Japan). Band intensities were digitized and quantified using Multi-gauge (Fujifilm, Tokyo, Japan). Exon 22 inclusion rate (*SERCA1a* percentage) was represented as normal band percentage. Statistical analysis was performed using GraphPad Prism 4 (Graphpad Software, CA, USA).

2.2. RNA interference

For RNAi, siRNAs specific for PKC isozymes except PKCα were designed using BLOCK-iT™ RNAi Designer (Invitrogen, CA, USA). PKCα specific siRNA (SIGMA Genosys, Tokyo, Japan) was designed according to [21]. All siRNA (see sense-strand siRNA sequences in **Supplementary Table S1**) and negative control RNAi (Stealth™ RNAi Negative Control Low GC Duplex #2) were purchased from Invitrogen and transfected with RNAi MAX (Invitrogen, CA, USA) according to the manufacturer's procedure. Cells were cultured for 48 h after transfection. In the case of PMA treatment, PMA (500 nM) was added to the medium 4 h after transfection.

To verify RNA interference, gene-specific primer sets [22–24] were used to amplify endogenous mRNA. Semi-quantitative RT-PCR or quantitative PCR (see primers and amplification conditions in **Supplementary Table S2–S4**) was performed. Quantitive PCR was performed with Power SYBR Green PCR Master Mix (Applied BioSystems) using a StepOnePlus™ Real Time PCR System (Applied Biosystems, CA, USA) according to the manufacturer's protocol.

3. Results

3.1. PMA regulates SERCA1 exon 22 splicing

To explore the relationship between PKC and *SERCA1* splicing, we first conducted reverse transcription polymerase chain reaction (RT-PCR) analysis to detect changes in splicing induced by PMA. PMA activates PKC when applied for a short period of time and acts as a PKC downregulator when applied for longer periods of time. As PKC is usually in an inactivated (dephosphorylated) state in cells [25], PMA was considered as an idle compound to explore the regulation of alternative splicing by PKC signaling. We assessed the splicing pattern of endogenous *SERCA1*. *SERCA1a* (3570 bp), which is a normal spliced variant, contains exon 22, while the abnormally spliced variant *SERCA1b* (3528 bp) lacks it. Exons 21–23 of *SERCA1* mRNA were amplified (*SERCA1a*, 240 bp; *SERCA1b*, 198 bp) (Fig. 1A). *SERCA1* is aberrantly spliced in DM1 patients and its splicing pattern is strictly regulated in individuals without DM1. This suggests that regulation of the alternative splicing of *SERCA1* may play a central role in the pathogenesis of DM1. However, the mechanism of *SERCA1* splicing remains to be elucidated.

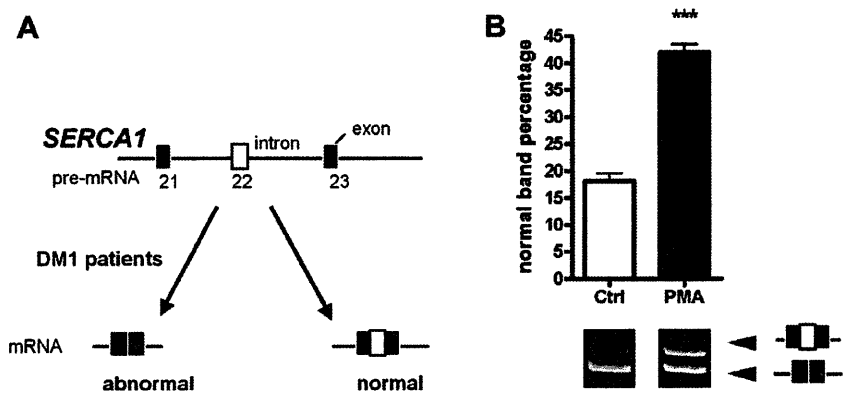

Fig. 1. PMA affects *SERCA1* splicing. (A) Schematic diagram showing two *SERCA1* splicing patterns. (B) RT-PCR analysis of the effects of treatment with 500 nM PMA for 48 h on endogenous *SERCA1* splicing as compared with DMSO (control). Significant differences: ***$P < 0.001$ (Student's *t*-test; mean ± SE; $n = 3$).

Applying 500 nM PMA for 48 h to downregulate PKC in HEK293 cells significantly improved *SERCA1a* splicing (Fig. 1B). It was previously shown that the PKC inhibitor Ro 31-8220 normalized DM1 abnormalities [20], suggesting that downregulation of PKC by PMA led to a change in the *SERCA1* splicing pattern.

3.2. Time-course and dose-curve of PMA effects on SERCA1 exon 22 splicing

To further investigate the signaling pathway involved in the regulation of splicing by PMA, we conducted time-course and dose-curve PMA treatment experiments. Since PKC activation by PMA begins within 5 min [26–29], the time points were set to between 5 min and 72 h (5 min and 0.5, 1.5, 3, 10, 24, 48, and 72 h). After 48 h, normal splicing was increased (Fig. 2A). Promotion of normal splicing continued after 72 h. However, aberrant *SERCA1* splicing was significantly increased after 1.5 h (Fig. 2B). These results indicate dual regulation of alternative splicing of *SERCA1* by PMA.

In the dose-curve analysis, the effects of 5, 50, and 500 PMA were compared with a control (no PMA). The effects of PMA on *SERCA1* splicing at both 1.5 and 48 h were dose-dependent (Fig. 2C and D), supporting the idea that PMA regulates *SERCA1* splicing at both time points. In addition, as 500 nM PMA had the strongest effects on *SERCA1* splicing at both 1.5 and 48 h, subsequent PMA experiments were all conducted with a PMA concentration of 500 nM.

Based on these results, we predicted that PKC plays a critical role in *SERCA1* splicing. We hypothesized that PKC signaling regulates alternative splicing, its activation promotes aberrant splicing of *SERCA1*, and its inhibition or downregulation improves normal splicing of *SERCA1*.

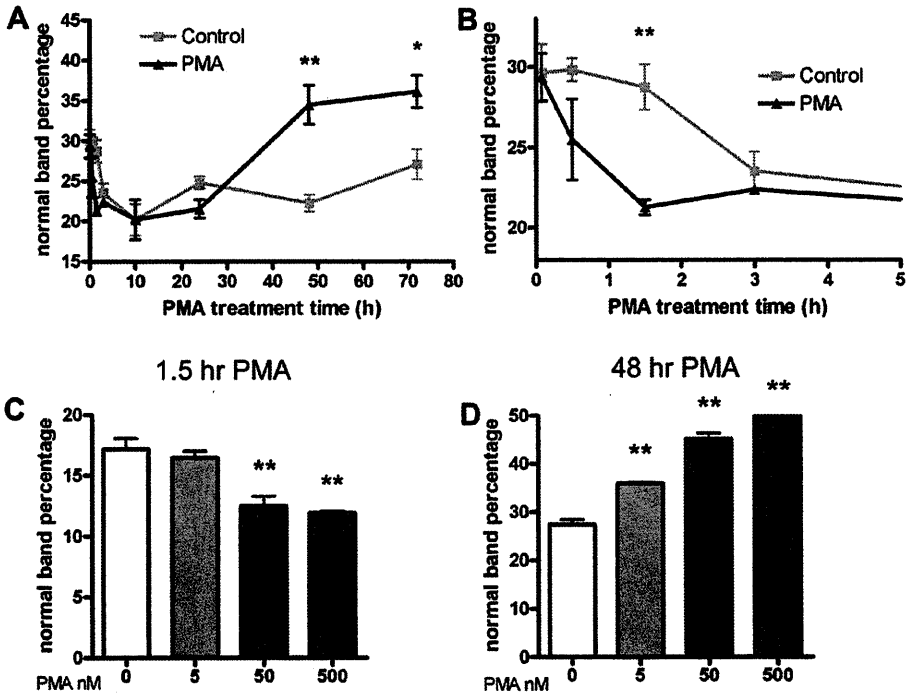

Fig. 2. Regulation of *SERCA1* splicing by PMA. RT-PCR analysis of endogenous *SERCA1* splicing. (A) Time-course of *SERCA1* splicing after stimulation with PMA (500 nM). (B) Data for the first 5 h of the time-course. Controls were treated with DMSO alone. Significant differences: *$P < 0.05$, **$P < 0.01$ (Student's *t* test; mean ± SE; $n = 3$). Dose-curve for the effect of PMA on *SERCA1* splicing (C and D). RT-PCR analysis of normally spliced endogenous *SERCA1* levels in HEK293 cells treated with 0 nM PMA (control) or 5, 50, or 500 nM PMA for 1.5 h (C) or 48 h (D). Significant differences: **$P < 0.01$ (Dunnett's test; mean ± SE; $n = 3$).

3.3. PKC regulates SERCA1 exon 22 splicing

To confirm the involvement of PKC signaling in the response to PMA treatment, the effects of co-treatment with PMA and the PKC inhibitor Ro 31-8220 were examined. Concurrent treatment with Ro 31-8220 (1 μM) completely abolished the effect of PMA treatment (500 nM) for 1.5 h; the level of normally spliced *SERCA1* was upregulated to the same level as in the control (Fig. 3A). Treatment with Ro 31-8220 alone promoted normal *SERCA1* splicing. The effect of PMA (500 nM) at 48 h was completely blocked by Ro 31-8220 (1 μM) (Fig. 3B). Based on these results, we conclude that downregulation of PKC leads to the promotion of *SERCA1a* splicing at 48 h. As 12 PKC isozymes with different functions in different signal transduction pathways have been identified to date, we hypothesized that one or more specific PKC isozymes are involved in the regulation of *SERCA1* splicing.

3.4. Suppression of PKCβII and PKCθ improves SERCA1a splicing

PMA normalizes *SERCA1* splicing, but multiple PKCs (cPKCs and nPKCs) with DAG binding motifs (C1A and C1B sites) can be activated or downregulated (after prolonged stimulation) by PMA. Hence, conventional and novel PKC isozymes may be involved in the regulatory effect of PMA on *SERCA1* splicing. Since aPKCs do not respond to DAG, they can be excluded as candidates. We sought to determine which of the cPKC or nPKC isozymes respond to treatment with PMA for 48 h and improve the production of normal *SERCA1* transcripts. Using RNA interference, we selectively suppressed PKC isozymes and determined whether knockdown of specific isozymes could mimic prolonged PMA stimulation (Fig. 4). Suppression of PKCβII and PKCθ increased normal *SERCA1* splicing, similar to stimulation with PMA for 48 h, while suppression of other PKC isozymes did not affect *SERCA1* splicing. Based on these results, we conclude that depletion of PKCβII and PKCθ improves *SERCA1a* splicing in HEK293 cells.

4. Discussion

In this study, we clarified the mechanism underlying PKC-mediated regulation of *SERCA1* splicing abnormalities in DM1. First, we identified PMA, a widely-used PKC activator and downregulator of PKC during prolonged stimulation, as a compound that effectively normalizes *SERCA1* splicing in HEK293 cells. By examining the properties of PMA's regulatory effects on *SERCA1* splicing, we found that PMA improved normal splicing during treatment for 48 h, while it increased aberrant splicing at 1.5 h. Two peaks for the effects of PMA on *SERCA1* splicing were confirmed to be dose-dependent. We then attempted to determine whether PKC is involved in PMA stimulation using the PKC inhibitor Ro 31-8220. Ro 31-8220 abolished the effects of PMA at both 1.5 and 48 h. However, treatment with Ro 31-8220 alone for 48 h did not affect splicing at all. This may be due to self-inhibition of PKC, meaning that Ro 31-8220 could not inhibit PKC, leaving *SERCA1* splicing unchanged. We thus confirmed the involvement of PKC in the regulation of *SERCA1* splicing by PMA.

The alternative splicing of several genes, including *Bcl-x*, *Axl* [30], and *CD45* [31], has have been reported to be affected by PKC-mediated phosphorylation. In addition, the connection between PKC and splicing-related factors (PSF, hnRNP A3, p68 RNA helicase, and hnRNP L) supports the idea that PKC regulates alternative splicing [32]. However, no specific PKC isozyme has been identified as a splicing regulator.

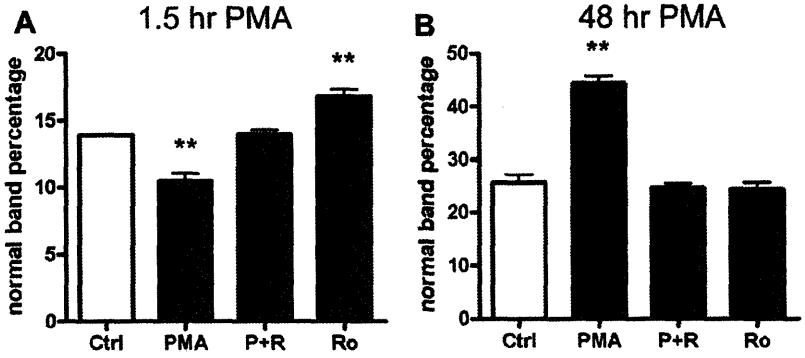

Fig. 3. PMA regulates *SERCA1* splicing via a PKC pathway. RT-PCR analysis of endogenous *SERCA1* splicing in HEK293 cells. PMA and the PKC inhibitor Ro 31-8220 were co-administered for 1.5 h (A) or 48 h (B). Controls were treated with DMSO alone. P = PMA (500 nM); R, Ro = Ro 31-8220 (1 μM). Significant differences: $^{**}P < 0.01$ (Dunnett's test; mean ± SE; $n = 3$).

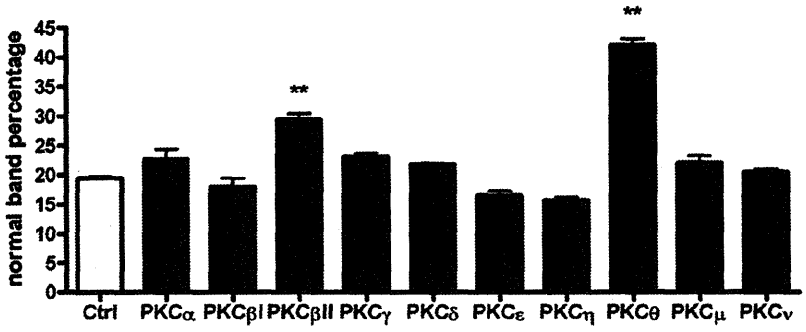

Fig. 4. RNA interference of PKC isozymes mimicked PMA regulation of *SERCA1* splicing. RT-PCR analysis of normally spliced endogenous *SERCA1* in HEK293 cells. RNAi specific for PKC isozymes (PKCα, PKCβI, PKCβII, PKCγ, PKCδ, PKCε, PKCη, PKCθ, PKCμ, or PKCν) as compared with control siRNA. Significant differences: $^{**}P < 0.01$ (Dunnett's test; mean ± SE; $n = 3$).

PKC is known to be involved in many diseases, including cancer, Alzheimer's disease, autoimmune diseases, and cardiovascular diseases. The association between the pathogenesis of DM1 and PKC was mentioned in previous reports [19,20], and CUGBP1 is the key to this association. Hyperphosphorylation of CUGBP1 has been confirmed in DM1 tissues, cells, and model mice and promotes an increase in the steady-state levels of CUGBP1. PKC activation is required for this hyperphosphorylation. Specifically, PKCα and PKCβII have been shown to directly activate CUGBP1 *in vitro* [19]. Furthermore, administration of the PKC inhibitor Ro 31-8220 to DM1 model mice ameliorated cardiac conduction defects [20]. These reports are consistent with our finding that PMA regulates the alternative splicing of *SERCA1* via a PKC pathway.

By selectively reducing the expression of PKC isozymes with siRNA, we identified PKCβII and PKCθ as isozymes that mimic 48 h PMA treatment. These two PKC isozymes promote production of the aberrant isoform *SERCA1b*. PKCθ is mainly expressed in skeletal muscle and T cells, which suggests that it plays crucial roles in myogenesis and the immune system [33,34]. Very recently, abolishing PKCθ in *mdx* (DMD model) mice was shown to prevent muscle wasting and improve muscle regeneration, maintenance, and performance [35]. DMD and DM1 are both progressive muscular dystrophies that have multiple symptoms in common (muscle weakness and muscular atrophy). Similar to DMD, our results showing that reductions in endogenous PKCθ levels in HEK293 cells induced normal *SERCA1* splicing in DM1 suggest that PKCθ is a candidate pharmacological therapeutic target in DM1. PKCβII, a Ca^{2+}-dependent isozyme, was shown to be involved in PMA-mediated CUGBP1 hyperphosphorylation, which induced DM1-like splicing abnormalities in a previous study[20]. So, we hypothesize that CUGBP1 may respond to PMA-induced PKC signaling. Interestingly, however, there were two discrepancies in the response of CUGBP1 to PKC signaling in the regulation of *SERCA1* splicing. First, CUGBP1 was previously shown to have no direct effect on *SERCA1* splicing [4], as demonstrated by overexpression of CUGBP1 in HEK293 cells and deduced from the observation of altered splicing of the *SERCA1* minigene and of endogenous *SERCA1* in C2C12 primary murine myoblast cells. The other difference is that CUGBP1 hyperphosphorylation peaks 3 h after PMA treatment [19]. This is 1.5 h after our *SERCA1* splicing pattern. We are going to check this issue by multiple methods: silencing endogenous CUGBP1 expression and overexpress recombinant CUGBP1, or other CELF families. Unfortunately, the slight but significant effect of stimulation with PMA for 1.5 h prevented us from identifying the PKC isozymes that respond to treatment with PMA for 1.5 h using siRNA.

To summarize, this is the first report to show that PKCβII and PKCθ are involved in the regulation of *SERCA1* alternative splicing. Note that PKCθ has not been reported to be involved in the regulation of alternative splicing. These findings suggest the existence of a neo-alternative splicing regulation pathway that operates via PKC. In conclusion, we not only identified novel potential therapeutic targets for DM1 treatment, but also showed the existence of a new alternative splicing regulatory mechanism.

Acknowledgments

We thank Drs. Y. Kino, K. Kanno, and Y. Nagara for valuable discussions. This work was supported by intramural research Grants (23-5) for Neurological and Psychiatric Disorders from the NCNP, Ministry of Health, Labour and Welfare, Japan.

Appendix A. Supplementary data

Supplementary data associated with this article can be found, in the online version, at http://dx.doi.org/10.1016/j.bbrc.2012.05.033.

References

[1] L.P. Ranum, J.W. Day, Myotonic dystrophy: RNA pathogenesis comes into focus, Am. J. Hum. Genet. 74 (2004) 793–804.
[2] A. Mankodi, M.P. Takahashi, H. Jiang, et al., Expanded CUG repeats trigger aberrant splicing of ClC-1 chloride channel pre-mRNA and hyperexcitability of skeletal muscle in myotonic dystrophy, Mol. Cell 10 (2002) 35–44.
[3] T.H. Ho, B.N. Charlet, M.G. Poulos, et al., Muscleblind proteins regulate alternative splicing, EMBO J. 23 (2004) 3103–3112.
[4] S. Hino, S. Kondo, H. Sekiya, et al., Molecular mechanisms responsible for aberrant splicing of SERCA1 in myotonic dystrophy type 1, Hum. Mol. Genet. 16 (2007) 2834–2843.
[5] R.N. Kanadia, K.A. Johnstone, A. Mankodi, et al., A muscleblind knockout model for myotonic dystrophy, Science 302 (2003) 1978–1980.
[6] M. Hao, K. Akrami, K. Wei, et al., Muscleblind-like 2 (Mbnl2) -deficient mice as a model for myotonic dystrophy, Dev. Dyn. 237 (2008) 403–410.
[7] A. Mykowska, K. Sobczak, M. Wojciechowska, et al., CAG repeats mimic CUG repeats in the misregulation of alternative splicing, Nucleic Acids Res. 39 (2011) 8938–8951.
[8] T.M. Wheeler, K. Sobczak, J.D. Lueck, et al., Thornton, Reversal of RNA dominance by displacement of protein sequestered on triplet repeat RNA, Science 325 (2009) 336–339.
[9] S.A. Mulders, W.J. van den Broek, T.M. Wheeler, et al., Triplet-repeat oligonucleotide-mediated reversal of RNA toxicity in myotonic dystrophy, Proc. Nat. Acad. Sci. U.S.A 106 (2009) 13915–13920.
[10] J. Kurreck, Antisense technologies. Improvement through novel chemical modifications, Eur. J. Biochem. 270 (2003) 1628–1644.
[11] A. Nishida, N. Kataoka, Y. Takeshima, et al., Chemical treatment enhances skipping of a mutated exon in the dystrophin gene, Nat. Commun. 2 (2011) 308, http://dx.doi.org/10.1038/ncomms1306.
[12] D.A. O'Leary, L. Vargas, O. Sharif, et al., HTS-compatible patient-derived cell-based assay to identify small molecule modulators of aberrant splicing in myotonic dystrophy type 1, Curr. Chem. Genomics 4 (2010) 9–18.
[13] E.L. Logigian, W.B. Martens, R.T. Moxley IV, et al., Mexiletine is an effective antimyotonia treatment in myotonic dystrophy type 1, Neurology 74 (2010) 1441–1448.
[14] C. Toyoshima, M. Nakasako, H. Nomura, et al., Crystal structure of the calcium pump of sarcoplasmic reticulum at 2.6 A resolution, Nature 405 (2000) 647–655.
[15] E. Zádor, L. Mendler, M. Ver Heyen, et al., Changes in mRNA levels of the sarcoplasmic/endoplasmic-reticulum Ca(2+)-ATPase isoforms in the rat soleus muscle regenerating from notexin-induced necrosis, Biochem. J. 320 (1996) 107–113.
[16] E. Zádor, L. Dux, F. Wuytack, Prolonged passive stretch of rat soleus muscle provokes an increase in the mRNA levels of the muscle regulatory factors distributed along the entire length of the fibers, J. Muscle Res. Cell Motil. 20 (1999) 395–402.
[17] T.H. Ho, D. Bundman, D.L. Armstrong, et al., Transgenic mice expressing CUG-BP1 reproduce splicing mis-regulation observed in myotonic dystrophy, Hum. Mol. Genet. 14 (2005) 1539–1547.
[18] Z.Z. Tang, V. Yarotskyy, L. Wei, et al., Muscle weakness in myotonic dystrophy associated with misregulated splicing and altered gating of CaV1.1 calcium channel, Hum. Mol. Genet. 21 (2012) 1312–1324.
[19] N.M. Kuyumcu-Martinez, G.S. Wang, T.A. Cooper, Increased steady-state levels of CUGBP1 in myotonic dystrophy 1 are due to PKC-mediated hyperphosphorylation, Molecular Cell 28 (2007) 68–78.
[20] G.S. Wang, M.N. Kuyumcu-Martinez, S. Sarma, et al., PKC inhibition ameliorates the cardiac phenotype in a mouse model of myotonic dystrophy type 1, J. Clin. Invest. 119 (2009) 3797–3806.
[21] N. Irie, N. Sakai, T. Ueyama, et al., Subtype- and species-specific knockdown of PKC using short interfering RNA, Biochem. Biophys. Res. Commun. 298 (2002) 738–743.
[22] H. Sakai, M. Yamamoto, Y. Kozutsumi, et al., Identification of PKC isoforms expressed in human bronchial smooth muscle cell, J. Smooth Muscle Res. 45 (2009) 55–62.
[23] K.I. Nagata, Y. Okano, Y. Nozawa, Protein kinase C isozymes in human megakaryoblastic leukemia cell line, MEG-01: possible involvement of the isozymes in the differentiation process of MEG-01 cells, Br. J. Haematol. 93 (1996) 762–771.
[24] A. Hayashi, N. Seki, A. Hattori, et al., PKCnu, a new member of the protein kinase C family, composes a fourth subfamily with PKCmu, Biochim. Biophys. Acta. 1450 (1999) 99–106.
[25] J.W. Orr, A.C. Newton, Intrapeptide regulation of protein kinase C, J. Biol. Chem. 269 (1994) 8383–8387.
[26] G. Nowak, Protein kinase C mediates repair of mitochondrial and transport functions after toxicant-induced injury in renal cells, J. Pharmacol Exp. Ther. 306 (2003) 157–165.
[27] M.C. Meyer, P.J. Kell, M.H. Creer, et al., Calcium-independent phospholipase A2 is regulated by a novel protein kinase C in human coronary artery endothelial cells, Am. J. Physiol. Cell Physiol. 288 (2005) C475–C482.
[28] M.H. Disatnik, S.C. Boutet, C.H. Lee, et al., Sequential activation of individual PKC isozymes in integrin-mediated muscle cell spreading: a role for MARCKS in an integrin signaling pathway, J. Cell Sci. 115 (2002) 2151–2163.

[29] A. Di, X.P. Gao, F. Qian, et al., The redox-sensitive cation channel TRPM2 modulates phagocyte ROS production and inflammation, Nat. Immunol. 13 (2011) 29–34.
[30] T. Revil, J. Toutant, L. Shkreta, et al., Protein kinase C-dependent control of Bcl-x alternative splicing, Mol. Cell. Biol. 27 (2007) 8431–8441.
[31] K.W. Lynch, A. Weiss, A model system for activation-induced alternative splicing of CD45 pre-mRNA in T cells implicates protein kinase C and Ras, Mol. Cell Biol. 20 (2000) 70–80.
[32] U. Rosenberger, I. Lehmann, C. Weise, et al., Identification of PSF as a protein kinase Calpha-binding protein in the cell nucleus, J. Cell Biochem. 86 (2002) 394–402.
[33] S. Osada, K. Mizuno, T.C. Saido, et al., A new member of the protein kinase C family, nPKCθ, predominantly expressed in skeletal muscle, Mol. Cell Biol. 12 (1992) 3930–3938.
[34] G. Baier, D. Telford, L. Giampa, et al., Molecular cloning and characterization of PKCθ, a novel member of the protein kinase C (PKC) gene family expressed predominantly in hematopoietic cells, J. Biol. Chem. 268 (1993) 4997–5004.
[35] L. Madaro, A. Pelle, C. Nicoletti, et al., PKC theta ablation improves healing in a mouse model of muscular dystrophy, PLoS One 7 (2012) e31515, http://dx.doi.org/10.1371/journal.pone.0031515.

Journal of Neuroscience Research

Journal of Neuroscience Research 90:870–877 (2012)

Localization of Mature Neprilysin in Lipid Rafts

Kimihiko Sato,[1] Chiaki Tanabe,[2] Yoji Yonemura,[1] Haruhiko Watahiki,[1] Yimeng Zhao,[1] Sosuke Yagishita,[1] Maiko Ebina,[1] Satoshi Suo,[1] Eugene Futai,[1] Masayuki Murata,[1] and Shoichi Ishiura[1]*

[1]Department of Life Sciences, Graduate School of Arts and Sciences, The University of Tokyo, Tokyo, Japan

[2]Department of Neuroscience, School of Pharmacy, Iwate Medical University, Morioka, Japan

Alzheimer's disease (AD) is characterized by senile plaques caused by amyloid-β peptide (Aβ) accumulation. It has been reported that Aβ generation and accumulation occur in membrane microdomains, called *lipid rafts*, which are enriched in cholesterol and glycosphingolipids. Moreover, the ablation of cholesterol metabolism has been implicated in AD. Neprilysin (NEP), a neutral endopeptidase, is one of the major Aβ-degrading enzymes in the brain. Activation of NEP is a possible therapeutic target. However, it remains unknown whether the activity of NEP is regulated by its association with lipid rafts. Here we show that only the mature form of NEP, which has been glycosylated in the Golgi, exists in lipid rafts, where it is directly associated with phosphatidylserine. Moreover, the localization of NEP in lipid rafts is enhanced by its dimerization, as shown using the NEP E403C homodimerization mutant. However, the protease activities of the mature form of NEP, as assessed by in vitro peptide hydrolysis, did not differ between lipid rafts and nonlipid rafts. We conclude that cholesterol and other lipids regulate the localization of mature NEP to lipid rafts, where the substrate Aβ accumulates but does not modulate the protease activity of NEP.

Key words: Alzheimer's disease; neprilysin; lipid rafts

Alzheimer's disease (AD) is characterized by the formation of senile plaques, composed primarily of amyloid-β peptide (Aβ). Aβ deposition has been thought to cause neurofibrillary tangles, neuronal cell loss, vascular damage, and dementia (the amyloid hypothesis; Hardy and Higgins, 1992). It has recently been suggested that AD begins with hippocampal synaptic dysfunction caused by diffusible oligomeric assemblies of Aβ (Selkoe, 2002).

Aβ is produced from amyloid precursor protein (APP) by the action of β- and γ-secretases, although APP is usually cleaved within the Aβ sequence by α-secretase. Aβ is degraded by neprilysin (NEP; Iwata et al., 2001). NEP is a type II membrane metallopeptidase that is capable of degrading not only monomeric Aβ but also pathological oligomeric Aβ (Kanemitsu et al., 2003). It has been reported that NEP levels in the hippocampus and cortex decline with age (Iwata et al., 2002; Hellstrom-Lindahl et al., 2008). Thus, analysis of the mechanisms regulating NEP activity may provide valuable insights for new therapeutic targets.

Recently, there have been several reports on the activities of proteases being regulated by their localization to membrane microdomains, known as *lipid rafts*. Lipid rafts, which are enriched in cholesterol and glycosphingolipids, have been implicated in processes such as signal transduction, endocytosis, and cholesterol trafficking (Pike, 2004, 2006). Whereas α-secretase cleavage occurs in nonlipid rafts (Kojro et al., 2001; von Tresckow et al., 2004), Aβ generation occurs in lipid rafts (Wada et al., 2003). It has been reported that Aβ accumulation is initiated by its association with GM1 in lipid rafts (Matsuzaki et al., 2007) and that NEP is partially localized in lipid rafts (Angelisova et al., 1999; Riemann et al., 2001; Kawarabayashi et al., 2004). However, whether the activity of NEP is regulated by its localization in lipid rafts is unknown.

Here we show that localization of glycosylated mature NEP in lipid rafts is regulated by its association with cholesterol. Moreover, we show with the NEP E403C homodimerization mutant that this localization is enhanced by its dimerization. Furthermore, we investigated the protease activities of mature NEP by an in vitro peptide assay. Unexpectedly, they were comparable in lipid rafts and nonlipid rafts. These findings suggest

Additional Supporting Information may be found in the online version of this article.

K. Sato and C. Tanabe contributed equally to this work.

Contract grant sponsor: Ministry of Education, Science, Sports, Culture, and Technology of Japan.

*Correspondence to: Shoichi Ishiura, Department of Life Sciences, Graduate School of Arts and Sciences, The University of Tokyo, 3-8-1 Komaba, Meguro-ku, Tokyo 153-8902, Japan.
E-mail: cishiura@mail.ecc.u-tokyo.ac.jp

Received 2 June 2011; Revised 17 August 2011; Accepted 24 August 2011

Published online 20 December 2011 in Wiley Online Library (wileyonlinelibrary.com). DOI: 10.1002/jnr.22796

that cholesterol regulates the localization of mature NEP in lipid rafts, where the substrate Aβ accumulates but apparently does not modulate the protease activity of NEP.

MATERIALS AND METHODS

Vectors and Constructs

Human neprilysin, NEP WT, was inserted into the pcDNA3.1-3 × FLAG vector (Invitrogen, Carlsbad, CA), thereby fusing triplet tandem repeats of FLAG tag to its N-terminus. The expression product of this construct will be referred to as FLAG-NEP WT. NEP E584V, carrying a catalytically inactive mutant E584V, and NEP E403C, carrying a homodimerization mutant, were subcloned into the pcDNA3.1-3 × FLAG vector, yielding FLAG-NEP E584V and FLAG-NEP E403C, respectively.

Antibodies

The following antibodies were purchased: anti-FLAG M2 (Sigma, St. Louis, MO); antiflotillin-1 and anticalnexin (BD Transduction Laboratories, Lexington, KY); anti-monoclonal NEP (Leica Microsystems); and HRP-conjugated anti-mouse IgG (Cell Signaling Technology, Beverly, MA).

Cell Culture and Transfection

HEK293 cells were cultured in DMEM (Sigma) supplemented with 10% fetal bovine serum (Sigma). They were maintained at 37°C in an atmosphere containing 5% CO_2 in a tissue culture incubator. DNA transfection was performed by lipofection with FuGENE 6 Transfection Reagent (Roche, Indianapolis, IN) when cells were 50% confluent. Then, 24 hr later, cells were harvested or used in assays.

Isolation of the Membrane Fraction

Cells were dissolved in TBS (0.1 M Tris-HCl, pH 8.0, 150 mM NaCl) containing Complete, EDTA-free protease inhibitor (Roche) and 0.7 μg/ml pepstatin A (Sigma) and disrupted by passage 20 times through a 21-G needle. The cell sample was then centrifuged (2,000 rpm, 2 min, 4°C). The resulting supernatant was then centrifuged again (49,000 rpm, 30 min, 4°C; Optima MAX-E ultracentrifuge; Beckman Coulter). The pellet formed was dissolved in TBS containing Complete, EDTA-free protease inhibitors, 0.7 μg/ml pepstatin A, and 1% Triton X-100; incubated on ice for 1 hr; and ultracentrifuged again. The resulting supernatant will be referred to as the *membrane fraction*.

Enzymatic Deglycosylation

The membrane fraction was solubilized with 1% Triton X-100 and then deglycosylated through treatment with the following: 1) endoglycosidase H (endo H; BioLabs), according to the manufacturer's instructions, and 2) 1 U N-glycosidase F (Endo F; Roche) per 45 μg of protein. The membrane fraction was denatured by boiling for 3 min in 1% SDS and 2-mercaptoethanol (ME), suspended in a reaction buffer (50 mM EDTA, 1% 2-ME, 0.5% Triton X-100, 0.1% SDS, 1 U N-glycosidase F) containing Complete, EDTA-free protease inhibitors and 0.7 μg/ml pepstatin A and incubated at 37°C overnight.

Isolation of Lipid Rafts by Sucrose Density Gradient Centrifugation

Cells were lysed on ice in MBS buffer (25 mM MES, pH 6.5, 150 mM NaCl) containing 1% Triton X-100, Complete, EDTA-free protease inhibitors, and 0.7 μg/ml pepstatin A. Cell disruption was achieved by passing the lysate 10 times through a 21-G needle and then 20 times through a 27-G needle. The lysate was incubated at 4°C for 30 min, and an equal amount of 80% sucrose was then added to it. The sample and sucrose buffer, containing 5–40% sucrose, were sequentially loaded to the bottom of a tube and then centrifuged (36,000 rpm, 18 hr, 4°C; CP 70 WX ultracentrifuge; Hitachi). Fractions were collected from the top to the bottom. Equal volumes of these samples were analyzed by Western blotting.

Methyl-β-Cyclodextrin Treatment

HEK293 cells overexpressing FLAG NEP-WT were washed with PBS, treated with 10 mM methyl-β-cyclodextrin (MβCD; Trappsol) for 20 min in a CO_2 incubator at 37°C, and collected. Lipid rafts fractions were treated with 50 mM MβCD on ice for 1 hr, dissolved in a double volume of TBS containing Complete, EDTA-free protease inhibitors and 0.7 μg/ml pepstatin A, and centrifuged (49,000 rpm, 1 hr, 4°C). The supernatants were removed and the pellets dissolved in TBS.

Western Blotting

Equal amounts of protein samples were separated by SDS-PAGE or Blue Native-PAGE and transferred to Immobilon-P PVDF membranes (Millipore, Billerica, MA). In the case of Blue Native-PAGE, the membranes were washed and destained using methanol. The membranes were soaked in PBS containing 5% nonfat dried milk and 0.05% Tween for 1 hr and then incubated overnight at 4°C with primary antibodies diluted in PBS containing 0.05% Tween, 0.1% BSA, and 1 mM NaN_3. After washing, the membranes were incubated with HRP-conjugated secondary antibody for 1 hr. Antigen–antibody complexes were detected by enhanced chemiluminescence using a LAS-3000 Luminescent Image Analyzer (Fujifilm). Signals were quantified in MultiGauge software (version 2.3; Fujifilm).

Assay of NEP-Dependent Neutral Endopeptidase Activity

NEP activity was measured in vitro by incubation at 37°C for 1 hr in 100 mM MES (pH 6.8) containing Complete, EDTA-free protease inhibitors, 10 μM Z-Leu-Leu-Leu-H, and as a substrate 50 μM Z-Ala-Ala-Leu-*p*-nitroanilide (ZALL-*p*-NA; Peptide Institute), in the presence or absence of 10 μM thiorphan, a specific inhibitor of NEP.

Interaction of NEP With Various Lipids

Lipid-spotted membrane (P-6002; Echelon Biosciences) was treated with TBS containing 1% skim milk and gently

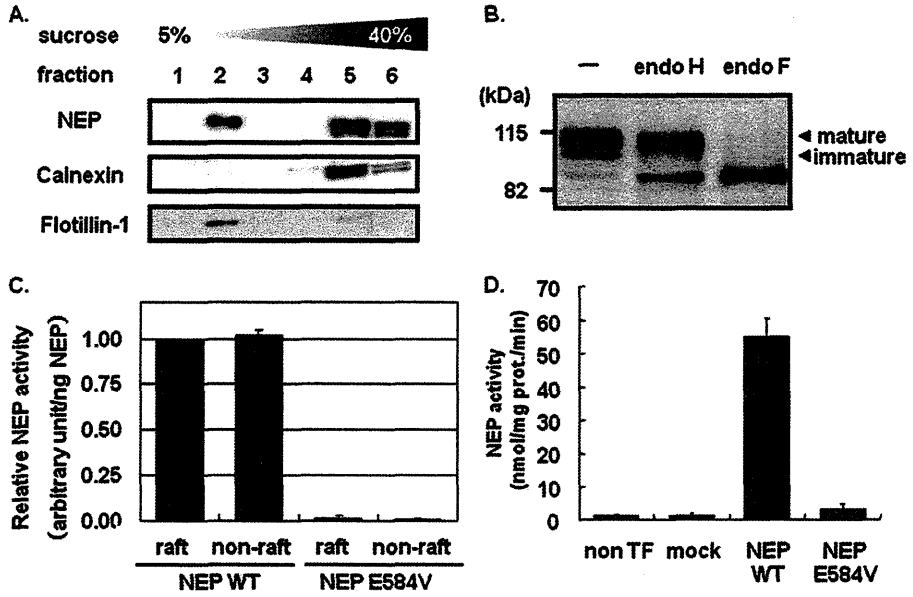

Fig. 1. NEP localization and activity in lipid rafts. **A:** Western blot analysis of lipid rafts fractionated from HEK293 cells overexpressing FLAG-NEP WT by a sucrose density-gradient centrifugation method. An anti-FLAG antibody was used to detect NEP. Lipid rafts were detected using an antibody raised against the raft marker flotillin-1. Nonlipid rafts (fraction 5) were detected using an antibody raised against the nonraft marker calnexin. **B:** Deglycosylation of the membrane fraction prepared from HEK293 cells overexpressing FLAG-NEP WT. The membrane fraction was treated with endoglycosidase H (endo H) and endoglycosidase F (endo F) or left untreated as a control (–), and then analyzed by Western blotting with an anti-FLAG antibody. **C:** Comparison of the specific enzymatic activity of the mature form NEP in lipid rafts (fraction 2) and nonlipid rafts (fraction 5), as assessed by *p*-NA peptide assay. Values represent the mean ± SD of three experiments. **D:** Neprilysin-dependent neutral endopeptidase activity in membrane fractions prepared from nontransfected HEK293 cells (non-TF) and cells transfected with vector (mock), FLAG-NEP WT (NEP WT) or the catalytically inactive mutant FLAG-NEP E584V. Values represent the mean ± SD of three experiments.

agitated for 1 hr at room temperature. SH-SY5Y neuronal cells were fractionated by sucrose density gradient centrifugation as shown previously, and each fraction was added to an equal volume of TBS containing protease inhibitor cocktail. After centrifugation at 49,000 rpm for 1 hr, the precipitate was dissolved in TBS containing protease inhibitor cocktail and incubated with the P-6002 membrane for 1 hr at room temperature. After incubation, the membrane was washed with TBS containing 0.1% Tween three times and incubated with anti-NEP monoclonal antibody diluted 1:2,000 for 1 hr at room temperature. The bound NEP was detected with an ECL advance kit (GE Healthcare, Amersham, United Kingdom).

RESULTS

Localization and Peptidase Activity of NEP in Lipid Rafts

To evaluate the peptidase activity of NEP in lipid rafts, we fractionated lipid rafts by sucrose density gradient centrifugation. We analyzed the localization of membrane-bound NEP extracted from HEK293 cells overexpressing FLAG-NEP WT. A raft marker, flotillin-1, was detected in fraction 2 and a nonraft marker, calnexin, in fractions 5 and 6 (Fig. 1A). FLAG-NEP was detected as a single band in fraction 2 and doublet bands in fractions 5 and 6. To distinguish these doublet bands, we deglycosylated the membrane fraction by treating it with endoglycosidase H (endo H) and endoglycosidase F (endo F; Fig. 1B). Although the upper band, the mature form, was resistant to endo H treatment, the lower band was deglycosylated by endo H. We will refer to the latter as the *immature form* of NEP. Resistance to endo H is acquired on transport of the protein to the Golgi apparatus, and this glycosylation is important for the catalytic activity of NEP (Lafrance et al., 1994). We compared the specific enzymatic activity of the mature form of NEP in lipid rafts (fraction 2) and nonlipid rafts (fraction 5); the contents of mature NEP were equalized by densitometric measurement of mature NEP levels after immunoblotting with an anti-FLAG antibody. The NEP activities of fractions 2 and 5, as assessed by *p*-NA peptide assay, were comparable (Fig. 1C). In this assay, catalytically inactive NEP E584V was used as a negative control (Fig. 1D).

Localization of NEP in Lipid Rafts Is Dependent on Cholesterol

Only mature NEP was detected in lipid rafts (Fig. 1A). We thus hypothesized that cholesterol in lipid rafts regulated the localization of mature NEP. To test this, we depleted HEK293 cells overexpressing FLAG-NEP

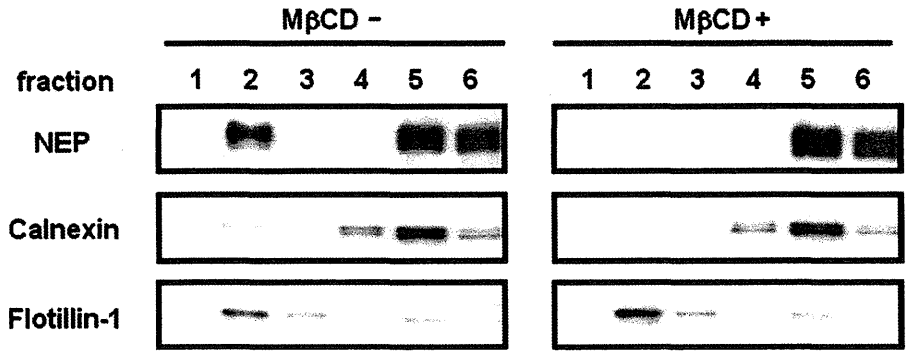

Fig. 2. Delocalization of NEP from lipid rafts in cells treated with MβCD. HEK293 cells overexpressing FLAG-NEP WT were treated with methyl-β-cyclodextrin (MβCD; +) or left untreated (–), and lipid rafts were fractionated as described in Materials and Methods.

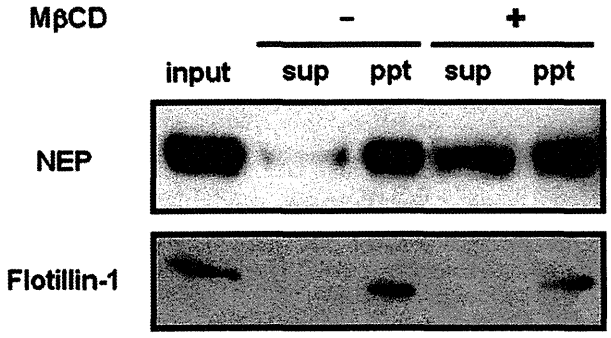

Fig. 3. Delocalization of NEP from fractionated lipid rafts after MβCD treatment. The lipid raft fraction, isolated from HEK293 cells overexpressing FLAG-NEP WT, was treated with (+) MβCD or left untreated (–) and separated into a supernatant (Sup) and a pellet (Ppt) by ultracentrifugation. The distribution of NEP was determined by Western blotting with an anti-FLAG antibody.

WT of cholesterol by treating them with 10 mM methyl-β-cyclodextrin (MβCD) for 20 min, and then fractionated the lipid rafts. More than 50% of cholesterol can be depleted from HEK293 cells by this treatment (Kojro et al., 2001). NEP became delocalized from lipid rafts following MβCD treatment, although flotillin-1 remained associated with them (Fig. 2).

We confirmed that the in vitro depletion of cholesterol from the lipid rafts fraction caused the delocalization of NEP from lipid rafts. We treated the fractionated lipid rafts with 50 mM MβCD for 1 hr at 4°C and separated them into supernatants and pellets by ultracentrifugation (Fig. 3). NEP and flotillin-1, associated with lipid rafts, were detected, as expected, in the pellets formed from lipid rafts not treated with MβCD. However, some of the NEP associated with lipid rafts was detected in supernatants prepared from lipid rafts treated with MβCD treatment. Flotillin-1 remained exclusively in the pellets, suggesting that flotillin-1 was not associated with choresterol.

Localization of NEP in Lipid Rafts Is Enhanced by Its Dimerization

To understand better the mechanism of NEP localization in lipid rafts, we investigated whether NEP dimerization facilitated the assembly of the enzyme in lipid rafts. We lysed HEK293 cells overexpressing FLAG-NEP WT in buffers containing different detergents and then analyzed NEP protein complexes by Blue Native-PAGE. Although NEP complexes were dissociated by NP-40 and Triton X-100, the 300-kDa complexes were resistant to treatment with DDM and digitonin (Fig. 4A). Next, we investigated the effect of dimerization on the localization of NEP in lipid rafts. It has been reported that rabbit NEP carrying an E403C mutation forms a covalent homodimer (Hoang et al., 1997). We introduced this mutation into human NEP and assessed its effect on the localization of NEP in lipid rafts. FLAG-NEP WT and FLAG-NEP E403C were detected as single 120-kDa bands after their separation by SDS-PAGE under reducing conditions (Fig. 4B). A 250-kDa FLAG-NEP E403C homodimer was detected under nonreducing conditions (Fig. 4B). These results indicate that, as in rabbit NEP, the E403C mutation caused human NEP to form of a covalent homodimer. Interestingly, although NEP WT complexes (Fig. 4A,C) were not resistant to Triton X-100, the NEP E403C mutant was resistant to Triton X-100 and formed a disulfide-bonded complex the same size as the NEP WT complex. Although we cannot exclude the possibility that the complex includes other proteins, the 300-kDa complex (Fig. 4A,C) appears to represent a covalent NEP homodimer.

Next, we compared the localization of mature forms of NEP WT and NEP E403C in lipid rafts. The ratio of the amount of mature NEP localized in lipid rafts to the total amount of mature NEP was 1.3 times higher in HEK293 cells overexpressing homodimeric mutant NEP E403C (47.7%) than in those expressing NEP WT (35.7%; Fig. 4D). These results demonstrate that the localization of NEP in lipid rafts was enhanced by its dimerization.

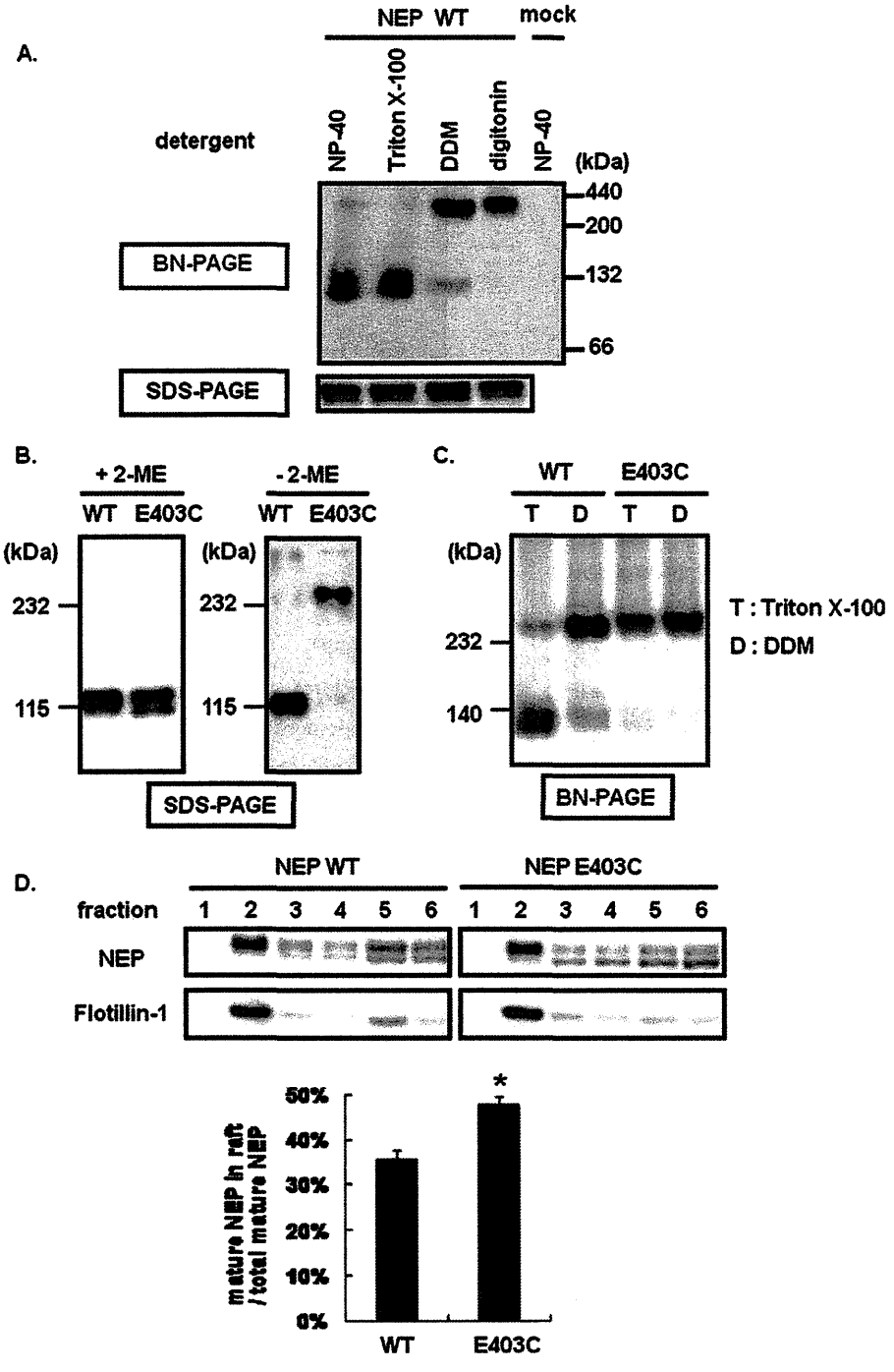

Fig. 4. Dimerization and localization of human NEP E403C in lipid rafts. **A:** Membrane fractions prepared from HEK293 cells overexpressing FLAG-NEP WT (NEP WT) or vector (mock) were dissolved in buffer containing detergents, such as NP-40, Triton X-100, DDM, and digitonin (all at a concentration of 1%). NEP complexes were analyzed by Blue Native-PAGE (BN-PAGE) or SDS-PAGE, followed by Western blotting with an anti-FLAG antibody. **B:** Membrane fractions obtained from HEK293 cells overexpressing FLAG-NEP WT (WT) or FLAG-NEP E403C (E403C) were analyzed by SDS-PAGE, performed with (**left**) or without (**right**) 2-ME. **C:** Membrane fractions obtained from HEK293 cells overexpressing FLAG-NEP WT (WT) or FLAG-NEP E403C (E403C) were dissolved in buffer containing 1% Triton X-100 (T) or 1% of DDM (D). The resulting lysates were analyzed by Blue Native-PAGE (BN-PAGE) and Western blotting with an anti-FLAG antibody. **D:** Effect of the E403C mutation on the distribution of NEP in lipid rafts. Lipid rafts from HEK293 cells overexpressing FLAG-NEP WT (NEP WT) or FLAG-NEP E403C (NEP E403C) were fractionated by sucrose density-gradient centrifugation and analyzed by Western blotting with an anti-FLAG antibody. The ratio of the amount of mature NEP localized in lipid rafts to the total amount of mature NEP was determined by densitometric measurement of protein bands corresponding to the mature form of NEP. Values represent the mean ± SD of three experiments. Statistical analysis was performed using a two-tailed Student's *t*-test. $\star P < 0.05$ was considered to indicate statistical significance (bottom graph).